Pharm Res (2014) 31:3323–3334
DOI 10.1007/s11095-014-1422-3

RESEARCH PAPER

Chitosan-Based Hybrid Nanocomplex for siRNA Delivery and Its Application for Cancer Therapy

Min-Hyo Ki • Ji-Eon Kim • Young-Nam Lee • Sang Myoung Noh • Sung-Won An • Hyun-Jong Cho • Dae-Duk Kim

Received: 28 February 2014 / Accepted: 12 May 2014 / Published online: 24 May 2014

ABSTRACT

Purpose Chitosan, a natural and biocompatible cationic polymer, is an attractive carrier for small interfering RNA (siRNA) delivery. The purpose of this study was to develop a chitosan-based hybrid nanocomplex that exhibits enhanced physical stability in the bloodstream compared with conventional chitosan complexes. Hybrid nanocomplexes composed of chitosan, protamine, lecithin, and thiamine pyrophosphate were prepared for systemic delivery of survivin (SVN) siRNA.

Methods Physicochemical properties of the nanoparticles including mean diameters and zeta potentials were characterized, and target gene silencing and cellular uptake efficiencies of the siRNA nanocomplexes in prostate cancer cells (PC-3 cells) were measured. *In vivo* tumor targetability and anti-tumor efficacy by systemic administration were assessed in a PC-3 tumor xenograft mouse model by near-infrared fluorescence (NIRF) imaging and tumor growth monitoring, respectively.

Results Mean diameters of the SVN siRNA-loaded hybrid nanocomplex (GP-L-CT) were less than 200 nm with a positive zeta potential value in water and were maintained without aggregation in culture media and 50% fetal bovine serum. SVN expression in PC-3 cells was reduced to 21.9% after treating with GP-L-CT. The tumor targetability and growth inhibitory efficacies of GP-L-CT supported the use of this novel hybrid nanocomplex as a cancer therapeutic and as a theranostic system for systemic administration.

Conclusions A chitosan-based hybrid nanocomplex was successfully developed for the systemic delivery of SVN siRNA, which could serve as an alternative to cationic polymeric nanoparticles that are unstable in serum.

KEY WORDS chitosan · lecithin · nanocomplex · protamine · survivin siRNA · thiamine pyrophosphate

ABBREVIATIONS

Cryo-TEM	Cryo-transmission electron microscopy
EPR	Enhanced permeability and retention
NIRF	Near-infrared fluorescence
RNAi	RNA interference
SCID	Severe combined immunodeficiency
siRNA	Small interfering ribonucleic acid
TPP	Thiamine pyrophosphate

INTRODUCTION

Various preclinical and clinical studies have been tried for the development of small interfering RNA (siRNA) therapeutics based on RNA interference (RNAi) technology (1). These studies have indicated that overcoming low cellular permeability of nucleic acids, as well as low stability against serum proteins and degradative enzymes, are prerequisites for therapeutic applications (2, 3). One of ways to solve these difficulties is the development of highly efficient nucleic acid delivery systems, which protect siRNA from nucleases presented in the body fluids, improve low cellular membrane permeability, and ameliorate endosomolysis (4).

Many strategies have been developed using non-viral vehicles for the delivery of RNAi (5). The primary approach has

Electronic supplementary material The online version of this article (doi:10.1007/s11095-014-1422-3) contains supplementary material, which is available to authorized users.

M.-H. Ki • Y.-N. Lee • S. M. Noh • S.-W. An
Chong Kun Dang Research Institute, Chong Kun Dang Pharm.
Yongin 446-916, Republic of Korea

H.-J. Cho
College of Pharmacy, Kangwon National University
Chuncheon 200-701, Republic of Korea

M.-H. Ki • J.-E. Kim • D.-D. Kim (✉)
College of Pharmacy and Research Institute of Pharmaceutical Sciences
Seoul National University, Seoul 151-742, Republic of Korea
e-mail: ddkim@snu.ac.kr

been the addition of cationic and lipophilic properties that overcome the limited cellular permeability of anionic and hydrophilic nucleic acids. Among these approaches, nucleic acid delivery systems based on cationic polymers and lipids has gained attention (6). Typical cationic polymers could be classified into synthetic polymers (i.e., polyethyleneimine, poly-L-lysine, poly-L-arginine) and natural polymers (i.e., chitosan) (7, 8). Chitosan has been widely used in the development of nucleic acid delivery systems due to its low cytotoxicity, high biocompatibility, and high cellular permeability (9). Its nucleic acid binding and delivery capacity can be influenced by its molecular weight and the degree of deacetylation (10, 11). Moreover, chitosan conjugated with a cationic polymer, peptide, and hydrophobic residue exhibits improved gene transfection efficiency (12–15), while the introduction of polyethylene glycol can increase chitosan hydrophilicity and stability in biological fluids (16).

However, clinical application and commercialization of synthetic chitosan conjugates could be hampered by toxicity of the delivery vehicle. Thus, a non-modified (i.e., natural) chitosan-based gene delivery system would be preferable if gene transfection efficiency could be maintained. Nevertheless, there are also some obstacles in using natural chitosan for siRNA delivery. Conventional siRNA delivery of cationic nanoparticles using chitosan can induce protein binding and aggregation in the bloodstream, resulting in peripheral vascular thrombosis and hemolysis as the surface charge increases (17–19). These phenomena in nanoparticle formulations can also influence the delivery accuracy and efficiency of therapeutics (20). Because of these reasons, few studies have described the intravenous administration of siRNA/chitosan nanoparticles until now (10, 21). In addition, even though chitosan may exhibit high binding affinity with siRNA due to its cationic charge density in acidic pH, the siRNA/chitosan complex tends to be physically unstable in neutral and basic pH conditions (22). These problems need to be solved through the optimal design of a stable chitosan-based nanocomplex in physiological conditions for successful siRNA delivery using natural chitosan.

Survivin (SVN) is an inhibitor of apoptosis and is thought to be a promising target for cancer therapy. It is minimally expressed in normal tissues and up-regulated in many cancers, including prostate cancer (23). Thus, SVN could be a good target protein for siRNA nanocomplex studies. In addition, several studies have shown that protamine, which binds to nucleic acids to form a stable nanocomplex via ionic and hydrophobic interactions, could be used for pre-complex preparation in the development of a nucleic acid nanocomplex (24–26). Herein, we thus prepared pre-complex with siRNA and protamine, which has a negative net charge for subsequent binding with cationic chitosan, by combining a limited amount of protamine. Phospholipid was then introduced into the siRNA/protamine pre-complex for the enhancement of nanocomplex stability in the bloodstream because protamine is known to have a binding affinity for the lipophilic moiety in a phospholipid (27, 28). In order to enhance the transfection efficiency of siRNA through the addition of a positive surface charge on this complex, chitosan was added together with thiamine pyrophosphate (TPP). TPP, combined with chitosan, is known to maintain the delivery efficiency of the siRNA/chitosan complex in neutral physiological pH, because the positively charged amine group of thiazolium in TPP stabilizes the complex regardless of the pH conditions (29). Following preparation of the nanoparticle complex, the physicochemical properties and siRNA delivery efficiency were assessed *in vitro* and *in vivo*.

MATERIALS AND METHODS

Materials

siRNA for SVN, luciferase, and Cy5.5-SVN (Cy5.5-siRNA) were provided by Bioneer Co. (Daejeon, Korea). Their sequences were as follows: SVN siRNA [sense: 5'-AAGGAG AUCAACAUUUUCA (dTdT)-3', anti-sense: 5'-UGAAAA UGUUGAUCUCCUU (dTdT)-3'], luciferase siRNA [sense: 5'-UUGUUUUGGAGCACGGAAA (dTdT)-3', anti-sense: 5'-UUUCCGUGCUCCAAAACAA (dTdT)-3']. Chitosan acetate and chitosan hydrochloride (HCl) were purchased from Heppe Medical Chitosan (Halle, Germany) and FMC BioPolymer (Philadelphia, PA, USA), respectively. BLOCK-iT fluorescent oligo and Lipofectamine 2000 (L2K) were obtained from Invitrogen (Carlsbad, CA, USA), and GelRed was acquired from Biotium, Inc. (Hayward, CA, USA). Lecithin, protamine, and TPP were purchased from Alps Pharmaceutical (Hida, Japan), Lipoid (Ludwigshafen, Germany), and Sigma-Aldrich (St. Louis, MO, USA), respectively. A human SVN Quantikine ELISA kit was obtained from R&D Systems (Minneapolis, MN, USA), and Matrigel was acquired from BD Biosciences (Bedford, MA, USA). Fetal bovine serum (FBS), penicillin, streptomycin, RPMI 1640 (developed at Roswell Park Memorial Institute), phosphate-buffered saline (PBS), Tris-borate-EDTA, and trypsin-EDTA were obtained from Gibco Life Technologies, Inc. (Grand Island, NY, USA). All other chemicals were of analytical grade.

Preparation of Hybrid Nanocomplex

Hybrid nanocomplexes were prepared by the combination of SVN siRNA, protamine, lecithin, chitosan, and TPP. Briefly, 10 mg of siRNA, 0.5 mg of protamine sulfate, 4 mg of chitosan HCl (150–400 kDa, FMC CL214, FMC BioPolymer, Philadelphia, PA, USA), and 20 mg of TPP were each solubilized

in 1 mL of diethylpyrocarbonate-treated distilled water (DW) and individually filtered. For lecithin (Lipoid S-100), 30 mg were dissolved in 1 mL of ethanol and filtered. The pre-complex was prepared by mixing and stirring SVN siRNA and protamine solutions. A lecithin solution was added into the pre-complex solution and stirred for 30 min. The final formulation, GP-L-CT, was prepared by adding chitosan and TPP solutions into the mixture. All components in the formulation were added and mixed according to weight ratios of the compositions. Other complexes were also prepared according to the manufacturing order of GP-L-CT. For siRNA/L2K complex as the control, a mixture of SVN siRNA (100 μg) and L2K (300 μL) was prepared and incubated for 20 min before use.

Particle Size and Zeta Potential Measurements

The mean diameter and zeta potential values of the developed complexes were measured by a light-scattering spectrophotometer (ELS-Z, Otsuka Electronics, Tokyo, Japan), according to the manufacturer's protocol. Complexes corresponding to 20 μg of siRNA were dispersed in DW (0.5 mL) for analysis. The stability of complexes was assessed in cell culture medium (RPMI 1640) and 50% (v/v) FBS. FBS was used after removing the flocculence (centrifugation at 400*g* and 0.2 μm filtration) according to the user's guide. Similarly, complexes corresponding to 20 μg of siRNA were diluted in 0.5 mL of cell culture medium and 50% FBS. After incubation for 3 h, the mean diameter and zeta potential values were measured by the ELS-Z system.

Cryo-Transmission Electron Microscopy (Cryo-TEM)

The morphology of the developed complexes was observed by cryo-TEM (Tecnai G2 F20 Cryo-TEM, FEI Company, Hillsboro, Oregon, USA) (30). The specimen was applied to holey carbon affixed to the grid (Quantifoil Micro Tools GmbH, Jena, Germany) and rapidly cooled to−170°C. It was fixed in the cryo-holder and inserted into the cryo-TEM at−170°C. Images were recorded under low electron dose conditions.

Gel Retardation Assays

Each sample was separated in a 2.5% agarose gel that included 0.001% GelRed in a Tris-borate-EDTA buffer at 50 V for 15 min. After electrophoresis, complex formation was evaluated by scanning with MiniBIS Pro (DNR Bio-imaging Systems, USA).

Quantification of Non-loaded Free siRNA

Non-loaded free SVN siRNA was assayed by high performance liquid chromatography (HPLC) after ultracentrifugation, to estimate loading amount of siRNA. Free SVN siRNA was separated from nanocomplexes by ultracentrifugation at 100,000*g* for 60 min at 15°C using Optimal-100XP ultracentrifuge (Beckman Coulter, Brea, CA, USA) (31). The free siRNA in the obtained supernatant was assayed using Waters Alliance 2695 HPLC system (Waters, Milford, MA, USA) and the Xterra® C18 column (5 μm, 4.6×150 mm, Waters, Milford, MA, USA). The mobile phase consisted of 100 mM triethylammonium acetate with pH 7.0 in water (MP-A) and acetonitrile (MP-B), and the flow rate was 0.5 mL/min. The gradient elution programs of the mobile phases were as follows: 93–90% MP-A; 7–10% MP-B, 0.0–30.0 min; 90–50% MP-A; 10–50% MP-B, 30.0–35.0 min; 50–20% MP-A; 50–80% MP-B, 35.0–40.0 min; 20–93% MP-A; 80–7%, 40.0–40.1 min; and 93% MP-A; 7% MP-B, 40.1–60 min. The samples were prepared by diluting 0.1 mL of the supernatant with 0.9 mL of MP-A. The standard were prepared by dissolving SVN siRNA to 30 μg/mL with MP-A. The sample or standard (10 μL each) was injected and detected by UV at a wavelength of 260 nm. The good linearity in a calibration curve of HPLC analysis was obtained at the concentration ranges of 1.0–100.0 μg/mL for anti-sense siRNA strands as demonstrated by the high correlation coefficient (R2) value of above 0.99 (Fig. S1).

In Vitro Transfection Study

For the *in vitro* transfection study, gene-silencing efficiency was evaluated in a human prostate cancer cell, PC-3, purchased from the Korea Cell Line Bank (KCLB; Seoul, Korea). Cells were cultured with RPMI 1640 containing 10% FBS, 100 U/mL penicillin, and 100 μg/mL streptomycin in a 5% CO_2 atmosphere with 95% relative humidity at 37°C. To evaluate gene-silencing efficiency, SVN expression (%) was measured by a human SVN Quantikine ELISA kit. In brief, PC-3 cells were seeded into a 6-well plate at a density of 1×10^5 cells/well and cultured for 48 h. Before loading the samples with SVN siRNA or luciferase siRNA as control, cells were stabilized for 2 h with fresh culture media. PC-3 cells were incubated with complexes corresponding to 2 μg of siRNA/well for 48 h in a 5% CO_2 atmosphere with 95% relative humidity at 37°C. Cells were lysed with the addition of 500 μL of cell lysis buffer (Cell Signaling Technology, Inc., Danvers, MA, USA) and collected. Cell lysates were centrifuged at 12,000 rpm for 20 min and 100 μL of the supernatant was used for the subsequent assay. Assay diluent (100 μL) and collected supernatant (100 μL) were mixed and stirred at 500 rpm for 2 h. Upon washing four times, the SVN conjugate (200 μL) was added and stirred for 2 h at room temperature. After washing additional four times, the substrate solution (200 μL) was added and incubated for 30 min in the dark. The reaction was terminated with the addition of stop solution (50 μL), and the absorbance at 450 nm was read by a SpectraMax M2

microplate reader (Molecular Devices, Sunnyvale, CA, USA). The amount (%) of SVN was calculated by substituting absorbance values into the regression line obtained from a standard solution. SVN expression rate was measured, regarding that of the untreated group as 100%. Gene-silencing efficiency was calculated according to following formula: efficiency = (1 − SVN expression rate in test group/SVN expression rate in control group) × 100.

In Vitro Cellular Uptake

Cellular uptake efficiency of siRNA was assessed by flow cytometry analysis (12). PC-3 cells were seeded onto 6-well plates at a density of 1×10^5 cells/well and incubated for 48 h in a 5% CO_2 atmosphere with 95% relative humidity at 37°C. All formulations were prepared using BLOCK-iT fluorescent oligo instead of SVN siRNA, as described above. PC-3 cells were incubated with naked siRNA (Naked) or complexes corresponding to 2 μg of BLOCK-iT fluorescent oligo/well for 24 h in a 5% CO_2 atmosphere with 95% relative humidity at 37°C. After incubating, cells were washed with PBS three times, and the fluorescence and optical photographs of cells were taken with the inverted microscope (Inverted Research Microscope ECLIPSE Ti, Nikon, Tokyo, Japan). Cells were collected by treatment with 0.25% trypsin-EDTA, and analyzed by flow cytometry (BD FACS Canto II; Becton-Dickinson, San Jose, CA, USA).

In Vivo Near-Infrared Fluorescence (NIRF) Imaging

The biodistribution of the complexes by systemic administration was assessed in a PC-3 tumor xenograft mouse model. Briefly, 2×10^6 PC-3 cells suspended in 50 μL of cell culture media with 50 μL of Matrigel were injected subcutaneously into 5-week-old male severe combined immunodeficiency (SCID) mice (Shizuoka Laboratory Animal Center, Hamamatsu, Japan). After attaining a tumor volume of 100 mm^3, complexes were injected intravenously via the tail vein at a dose of 80 μg siRNA (about 266 μL) per mouse. For NIRF imaging, Cy5.5-siRNA-loaded formulations were prepared using Cy5.5-siRNA instead of SVN siRNA, according to the method described above. NIRF images of the tumor region were obtained by the eXplore Optix system (Advanced Research Technologies-GE healthcare, St. Laurent, Quebec, Canada) at 2 and 5 h post-injection (32). Laser power and count time settings were 25 μW and 0.3 s per point, respectively. To excite the Cy5.5 molecules in the complexes, a laser diode at 670 nm was used.

In Vivo Anti-Tumor Efficacy

The PC-3 tumor xenograft mouse model was used to assess siRNA delivery efficiency of complexes of test or control groups. As described previously, 2×10^6 PC-3 cells suspended in 50 μL of cell culture media with 50 μL of Matrigel (BD Biosciences, Bedford, MA, USA) were injected subcutaneously into the 5-week-old male SCID mice. Luciferase siRNA was used as a irrelevant siRNA, and the preparation method of luciferase siRNA-loaded GP-L-CT was identical to that of SVN siRNA. After reaching a tumor volume of 100 mm^3, complexes corresponding to 40 μg siRNA (about 133 μL) per mouse were injected intravenously *via* the tail vein six times for 2 weeks. Tumor size was measured with Vernier calipers, and tumor volume and tumor inhibition rate (%) were calculated according to the following formula: $V = 0.5 \times \text{longest diameter} \times \text{shortest diameter}^2$; growth inhibition rate (%) = $[1 - (V_f - V_0 \text{ in test group})/(V_f - V_0 \text{ in control group})] \times 100$, where V_0 and V_f are the tumor volume at the initial day and final day tested, respectively.

Statistical Analysis

All experiments were conducted at least three times, and data are represented as means ± standard deviation (SD). Statistical analysis was based on analysis of variance (ANOVA).

RESULTS AND DISCUSSION

Determination of Nanocomplex Composition

To produce stable nanocomplexes without aggregation under physiological conditions *in vitro* and *in vivo*, optimal composition of the siRNA hybrid nanocomplexes was determined at each step in the preparation. All complex formulations were prepared according to the compositions presented in Table I. Protamine was introduced to form SVN siRNA/protamine pre-complexes and then chitosan + TPP was added to produce the SVN siRNA/chitosan/TPP complexes.

For the siRNA pre-complex formation, several weight ratios of siRNA and protamine were tested, ranging from 1:0.4 to 1:1 (w/w) (Table I). The pre-complexes with 1:0.4, 1:0.6, and 1:1 ratios had mean diameters of 261.9, 192.3, and 225.8 nm in DW, respectively, while the complex with a 1:0.8 ratio resulted in severe aggregation without measurable diameter and zeta potential values (Fig. 1a). Although it is not clear why aggregation was observed, a similar case was reported previously (33). The complexes with 1:0.4 and 1:0.6 ratios had negative surface charges according to zeta potential values and the complex with 1:1 converted to a positive surface charge. Thus, the amount of protamine in the pre-complex should be restricted to maintain the negative surface charge for the next step, which requires the addition of chitosan as a cationic polymer. The pre-complex with a 1:0.6 weight ratio

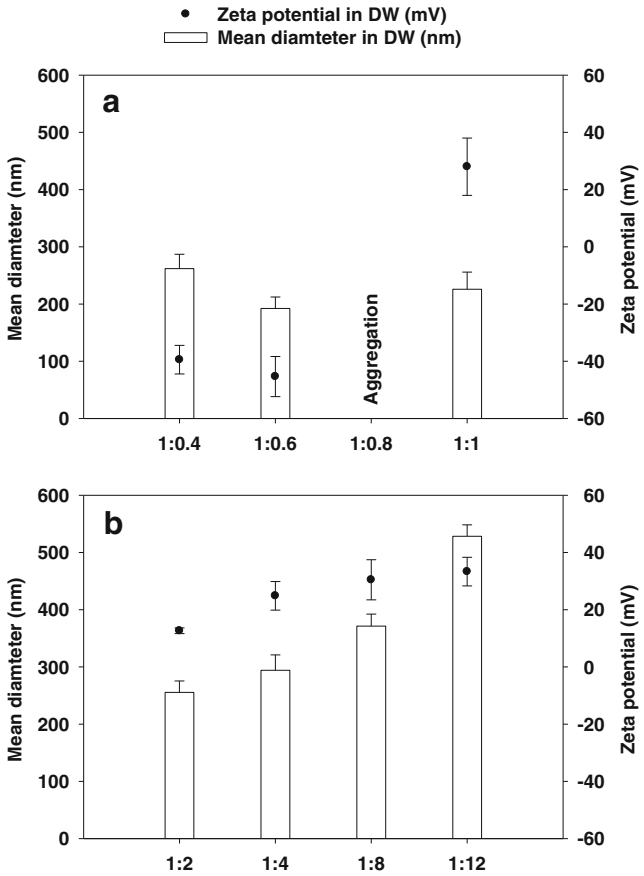

Fig. 1 Mean diameter and zeta potential values of siRNA/protamine pre-complexes and siRNA/chitosan/TPP complexes. (**a**) SVN siRNA/protamine pre-complexes with various siRNA:protamine ratios. (**b**) SVN siRNA/chitosan/TPP complexes with various siRNA:chitosan + TPP ratios. Chitosan + TPP was prepared at a ratio of 85/15 (w/w, %). Each value represents the mean ± SD ($n = 3$).

was selected for siRNA pre-complex formation because it showed the smallest diameter and a negative surface charge.

The mixture of chitosan and TPP (85:15, w/w) was used for complex formation with siRNA to complement the weak binding affinity of chitosan with siRNA in neutral physiological pH conditions (29). Several weight ratios of siRNA and chitosan + TPP were tested, ranging from 1:2 to 1:12 (w/w) corresponding to 3.5 to 21.1 of N/P (chitosan/siRNA) ratio (Table I). All siRNA/chitosan/TPP complexes had positive surface charges, reaching a plateau at a 1:8 ratio and showed larger mean diameters with increased amounts of chitosan + TPP (Fig. 1b). The complex of siRNA and chitosan + TPP with a 1:8 ratio was considered to be the optimal combination for efficient siRNA delivery because they had a high zeta potential value and relatively small mean diameter.

Based on these results, the siRNA pre-complex with siRNA and protamine (1:0.8, w/w) was subsequently complexed with chitosan + TPP at the 1:8 ratio of siRNA and chitosan + TPP. However, this resulted in a bulky complex with a mean diameter >600 nm. To ameliorate this phenomenon, lecithin was incorporated between the protamine pre-complex and chitosan complex steps, since protamine has a nanocomplex-stabilizing effect when it binds to the lipophilic moiety in a phospholipid (27, 28). The optimal lecithin amount was determined by comparing the mean diameters of the final nanocomplexes in DW, as well as in cell culture media and in 50% FBS. Lecithin was incorporated in ratios ranging from 1:5 to 1:15 (w/w) of siRNA and lecithin (Table II). The 1:10 ratio of siRNA and lecithin showed the smallest mean diameter nanocomplex compared with the 1:5 and 1:15 ratios in various media including serum conditions (Fig. 2). The mean diameter of the 1:10 ratio was 189, 129, and 181 nm in DW, culture media, and 50% FBS, respectively. However, that of the 1:15 ratio was 312, 340, and 404 nm, respectively, while that of the 1:5 ratio was >500 nm in DW and even larger in culture media and 50% FBS due to the aggregation. Therefore, we concluded that lecithin should be incorporated at no less than 10-fold the weight of the siRNA to stabilize the nanocomplex in culture media and 50% FBS. However, lecithin at a ratio >1:15 induced reversible bulky or loosened complexes that resulted in a slightly increased mean diameter. Therefore, the nanocomplex with the 1:10 ratio of siRNA and lecithin (GP-L-CT) was used as the final formulation and compared with comparative example formulations (Table III and Fig. 3) in further studies.

Before determination of the component compositions of the nanocomplex, the proper chitosan for siRNA delivery had been selected. Chitosan is a natural cationic polymer, which exists in a variety of molecular weights (MWs), salt types and deacetylation degrees. In our preliminary study, four chitosans with MWs of 50–400 kDa and 83–95% deacetylation degrees were tested (Table SI). The influences of chitosan MW and deacetylation on complex formation with SVN siRNA were investigated by gel retardation assay, as reported in the literature (34). Based on this result, chitosan D (chitosan HCl with a MW of 150–400 kDa and 95% deacetylation) exhibited higher siRNA-binding capability (Fig. S2) and resulted in lower SVN expression indicative of siRNA transfection efficiency, compared to other chitosans (Fig. S3). Therefore, chitosan D was selected and used for preparation of the chitosan-based complexes in the experiments.

Characterization of siRNA-Loaded Hybrid Nanocomplexes

The GP-L-CT nanocomplex (GP-L-CT) was prepared as described in Fig. 3 and the composition presented in Table III. The GP pre-complex (GP) was produced by mixing siRNA and protamine and the GP-L complex (GP-L) was produced by incorporating lecithin into GP. The final GP-L-CT was prepared by coating chitosan and TPP onto GP-L based on their electrostatic interaction. The morphology of GP, GP-L, and GP-L-CT was observed by cryo-TEM at each

Table I Composition of SVN siRNA/Protamine Pre-complexes and SVN siRNA/Chitosan/TPP Complexes

Components	siRNA:protamine (w/w)				siRNA:(chitosan + TPP) (w/w)			
	1:0.4	1:0.6	1:0.8	1:1	1:2	1:4	1:8	1:12
SVN siRNA	1	1	1	1	1	1	1	1
Protamine	0.4	0.6	0.8	1	-	-	-	-
Chitosan + TPP[a]	-	-	-	-	2	4	8	12

[a] Chitosan + TPP was prepared at a ratio of 85/15 (w/w, %).

All values are presented as weight ratios.

preparation step for the chitosan-based hybrid nanocomplex. As shown in Fig. 3a, GP had a reticular texture with a loosely disentangled particular shape. GP-L exhibited a partial reticular structure but showed a fused shape with a spherical liposome (Fig. 3b). In the case of GP-L-CT, the reticular texture completely disappeared and an opaque spot, characteristic of polymeric nanocomplexes, was presented (Fig. 3c). The cryo-TEM images demonstrated that the formation of tightly compacted nanocomplexes should be completed by complexing with cationic substances, chitosan and TPP, although the complexes could be stabilized by pre-complexing with protamine or lecithin incorporation processes. Other complex formulations were prepared for comparison with GP, GP-L, and GP-L-CT (Table III). As comparative examples, a G-C complex (G-C) was prepared by mixing siRNA and chitosan and a G-CT complex (G-CT) was made by mixing siRNA, chitosan and TPP. GP-CT complex (GP-CT) was produced using the same preparation method as GP-L-CT without lecithin incorporation.

The mean diameter and zeta potential values of the developed nanocomplexes in DW were measured and stability of the nanocomplexes was evaluated as the change in mean diameter in cell culture media and 50% FBS (Fig. 4). The mean diameters of GP, GP-L, and GP-L-CT in DW were 177, 133, and 189 nm, while those of G-C, G-CT, GP-CT as comparative examples were 377, 371, and 604 nm, respectively (Fig. 4a). Although FBS contained background signal of around 25 nm mean diameter (data not shown), the size measurement of nanocomplexes does not seem to be influenced by those smaller nanoparticles. Zeta potential values of GP and GP-L were negative due to the absence of the cationic substances, chitosan and TPP. In contrast, zeta potential values of GP-L-CT, G-C, G-CT, and GP-CT were positive due to the inclusion of chitosan, which is necessary for interaction with the negatively charged cellular membrane. Lecithin incorporation reduced the positive charge, seen when comparing the zeta potential value of GP-L-CT with that of GP-CT, due to lecithin itself having a slight negative charge. When the complexes were exposed to cell culture media and 50% FBS for 3 h, the complexes showed extremely different

Table II Composition of Chitosan-Based Hybrid Complexes with Lecithin Incorporation

Components	siRNA:lecithin (w/w)		
	1:5	1:10	1:15
SVN siRNA	1	1	1
Protamine	0.6	0.6	0.6
Lecithin	5	10	15
Chitosan	6.8	6.8	6.8
TPP	1.2	1.2	1.2

All values are presented as weight ratios.

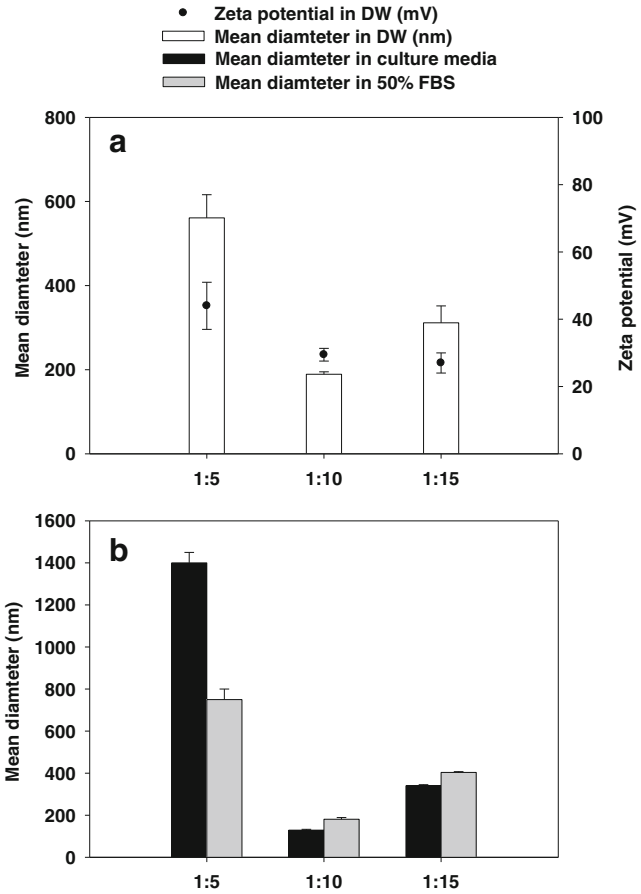

Fig. 2 Mean diameter and zeta potential values of chitosan-based complexes with various siRNA:lecithin ratios. (**a**) Mean diameters and zeta potentials of chitosan-based complexes with lecithin incorporation in DW. (**b**) Mean diameters of chitosan-based complexes with lecithin incorporation in culture media and 50% FBS. Each value represents the mean ± SD ($n = 3$).

Table III Compositions of SVN siRNA-Loaded Nanocomplexes and Comparative Examples

Components	GP	GP-L	GP-L-CT	G-C [a]	G-CT [a]	GP-CT [a]
SVN siRNA	1	1	1	1	1	1
Protamine	0.6	0.6	0.6	-	-	0.6
Lecithin	-	8	8	-	-	-
Chitosan	-	-	6.8	6.8	6.8	6.8
TPP	-	-	1.2	-	1.2	1.2

[a] G-C, G-CT, and GP-CT were prepared as comparative examples of GP-L-CT.

All values are presented as weight ratios.

changes in mean diameters. The mean diameters of GP, GP-L, and GP-L-CT were 25, 110, and 129 nm in culture media, and 33, 94, and 181 nm in 50% FBS, respectively (Fig. 4b). The mean diameters of G-C, G-CT, and GP-CT increased to >1,400 nm in culture media, and >1,000 nm in 50% FBS. The mean diameter of GP in culture media and 50% FBS was 20% smaller than that in DW and finally overlapped with the background signal of FBS (<30 nm), possibly due to dissociation of the complex. GP-L and GP-L-CT had a stable mean diameter, although it decreased slightly in culture media. In contrast, the mean diameters of G-C, G-CT, and GP-CT, which are conventional chitosan complexes that did not include protamine or lecithin, increased significantly with the precipitation of large particles in culture media and 50% FBS. GP-L-CT was more stable in the serum because of the formation of the liposomal complex (35, 36) as well as the reduction of the zeta potential (29.5 mV), compared to those of G-C, G-CT, and GP-CT (74.9–77.1 mV). Because the serum content in 50% FBS is similar to that in whole blood, G-C, G-CT, and GP-CT can form the aggregation *in vivo* that can result in the decrease of siRNA delivery efficiency and peripheral vascular thrombosis via intravenous injection.

When the influences of compositions on complex formation with SVN siRNA were investigated by gel retardation assay, GP-L-CT, G-C, G-CT, and GP-CT exhibited higher binding capabilities compared to GP and GP-L (Fig. 4c). It was supported by assay of non-loaded free siRNA using HPLC, in which GP and GP-L showed 31.7 ± 5.1 and 20.9 ± 2.9% of free siRNA, respectively, while other complexes had no detectable amount of free siRNA. To prepare a chitosan-based hybrid nanocomplex that can be systemically administered, GP-L-CT were evaluated with GP and GP-L as intermediate steps of GP-L-CT in further studies, excluding comparative examples such as G-C, G-CT, and GP-CT, which are physically unstable under physiological conditions.

In Vitro Gene Silencing and Cellular Uptake

In vitro gene silencing efficiency of the developed complexes was assessed by measuring SVN expression in PC-3 cells after incubating with SVN siRNA or luciferase siRNA as control for 48 h (Fig. 5). SVN expression rates were reduced to 7.0 and 21.9% by treatment with L2K and GP-L-CT containing SVN siRNA, while those were 68.5 and 105.5% with L2K and GP-L-CT containing luciferase siRNA, respectively. Thus, the gene silencing efficiencies of L2K and GP-L-CT were calculated as 89.8 and 79.2%, respectively. The high efficiencies were also supported by the siRNA-binding capacity of L2K and GP-L-CT exhibited in gel retardation assay (Fig. S4). Although L2K treatment resulted in higher gene silencing efficiency, its systemic application *in vivo* has been

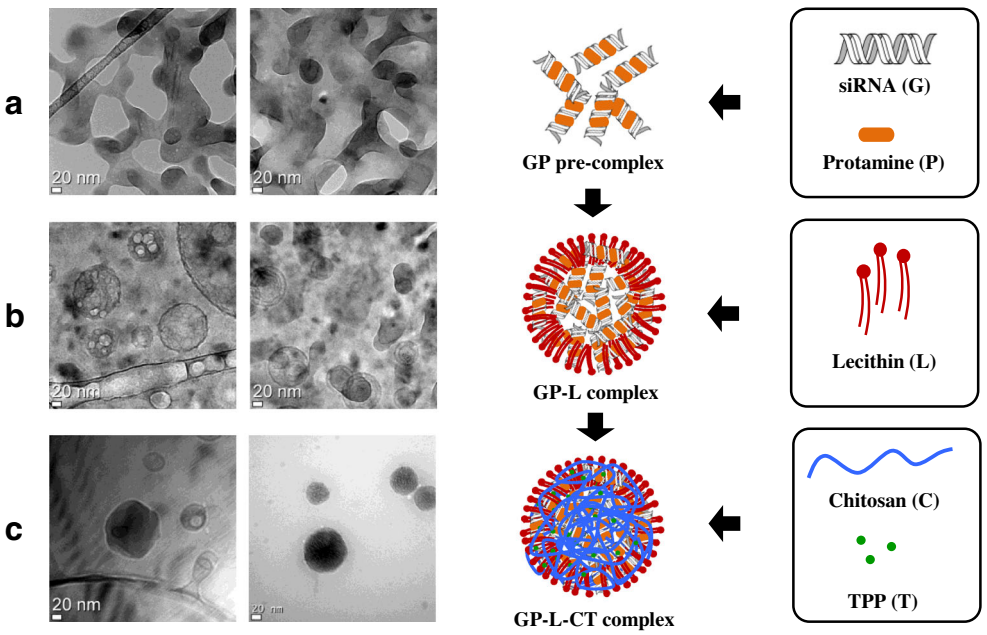

Fig. 3 Morphology of nanocomplex formulations observed by cryo-transmission electron microscopy (cryo-TEM) and schematic illustration of GP-L-CT hybrid nanocomplex preparation. Images of (**a**) siRNA/protamine pre-complex (GP), (**b**) siRNA/protamine/lecithin complex (GP-L), (**c**) siRNA/protamine/lecithin/chitosan/TPP complex (GP-L-CT) are presented. Scale bar = 20 nm.

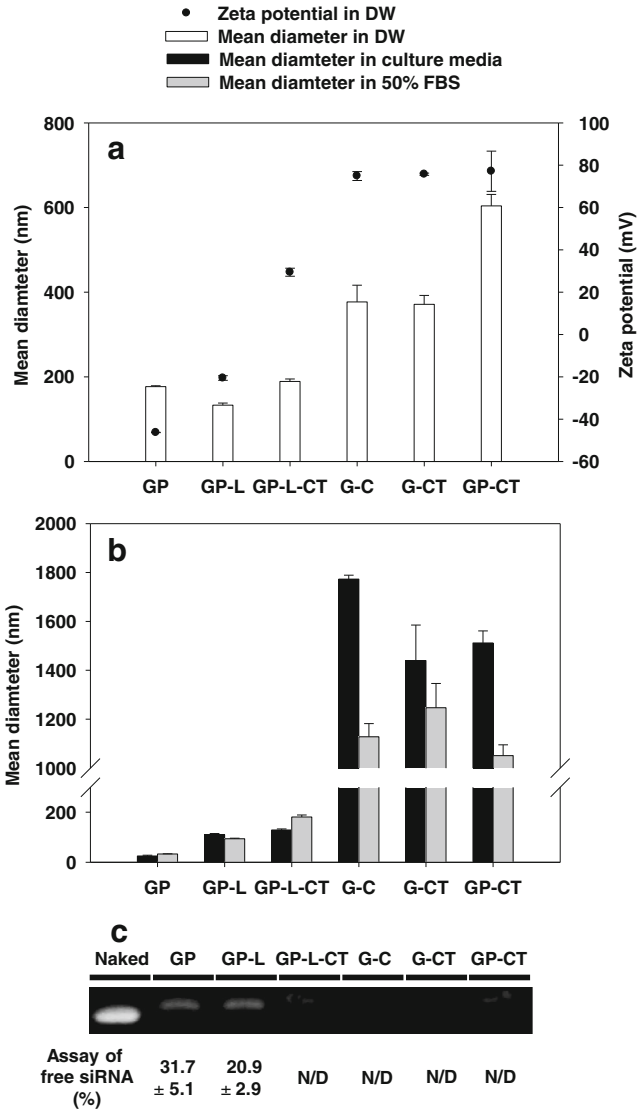

Fig. 4 Characterization of nanocomplex formulations by measurement of diameter and zeta potential values of complexes using a light-scattering spectrophotometer, gel retardation assay, and quantification of non-loaded free siRNA. The siRNA/protamine/lecithin/chitosan/TPP hybrid complex (GP-L-CT) was prepared through an intermediate step that included the siRNA/protamine pre-complex (GP) and siRNA/protamine/lecithin complex (GP-L). The siRNA/chitosan complex (G-C), siRNA/chitosan/TPP complex (G-CT), and siRNA/protamine/chitosan/TPP complex (GP-CT) were prepared as comparative examples of GP-L-CT. (**a**) Mean diameters and zeta potentials of chitosan-based nanocomplexes in DW are presented. (**b**) Mean diameters of chitosan-based nanocomplexes in culture media and 50% FBS are presented. (**c**) The gel retardation results by electrophoresis in 2.5% agarose gel and the quantified ratios of non-loaded free siRNA from complexes are presented. Each value represents the mean ± SD ($n = 3$).

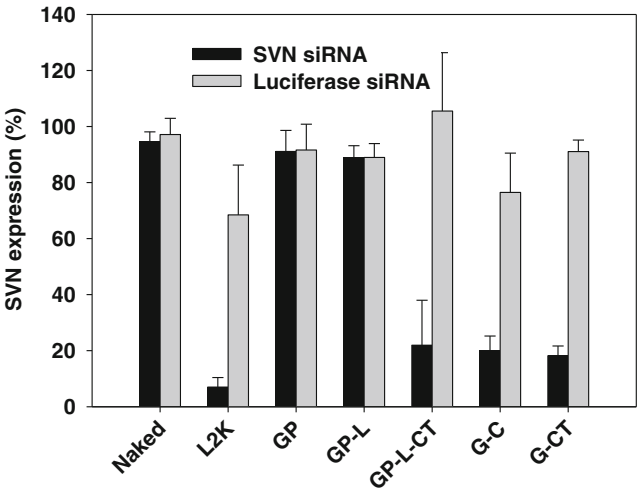

Fig. 5 *In vitro* transfection efficiency of SVN siRNA and luciferase siRNA-loaded complexes in PC-3 cells. SVN expression levels (%) following a 48-h transfection with naked siRNA (Naked), siRNA/Lipofectamine 2000 complex (L2K), siRNA/protamine pre-complex (GP), siRNA/protamine/lecithin complex (GP-L), siRNA/protamine/lecithin/chitosan/TPP complex (GP-L-CT), siRNA/chitosan complex (G-C) and siRNA/chitosan/TPP complex (G-CT)-incubated groups are presented. Each value represents the mean ± SD ($n = 3$).

restricted generally due to toxicity, which was implied by the decreased SVN expression rate in the control group (68.5%), as well as its low efficacy *in vivo* compared to *in vitro*. In the transfection study of conventional chitosan nanocomplexes, the gene silencing efficiencies of G-C and G-CT were 73.9% and 80.0%, respectively (Fig. 5), which means the efficiency of GP-L-CT was not reduced in spite of the composition of nanocomplex-stabilizing components, lecithin and protamine. In Naked, GP, and GP-L complexes that do not have cationic charges, SVN expression rates were not silenced at all, which indicates that complexes lacking a cationic moiety (i.e., chitosan and TPP) could not efficiently induce gene silencing. The control groups for Naked, GP, GP-L, and GP-L-CT complexes showed negligible cytotoxicity, which was supported by >90% SVN expression. Consequently, GP-L-CT was the most effective nanocomplex which induced *in vitro* gene silencing efficiency with SVN siRNA and did not decrease SVN expression rate with control siRNA indicating its low cytotoxicity.

Cellular uptake efficiency of developed complexes in PC-3 cells was evaluated by flow cytometry using complexes that included fluorescent siRNA (Fig. 6). The mean population percentages in P1 regions of L2K and GP-L-CT were 40.0 and 83.9%, respectively. A greater population shift into the P1 region is observed when more fluorescent siRNA is delivered into the cells through nanocomplexes. The mean population percentages in P1 regions of Naked, GP, and GP-L were 2.0, 3.3, and 2.8%, respectively, which indicates that the cells do not take up complexes without a cationic charge. Mean florescence intensity in Fig. 6 highly increased with GP-L-CT among the test groups, indicative of increased cellular uptake efficiency, which was also observed in dot plots by flow cytometry (Fig. S5). When the fluorescence and optical microscope images of cells on the well plate were taken after cellular uptake study, L2K and GP-L-CT showed fluorescent cell images by cellular uptake, while the Naked did not have fluorescence intensity (Fig. S6).

Based on a mean diameter <200 nm in serum and efficient gene silencing and cellular uptake, GP-L-CT was considered to

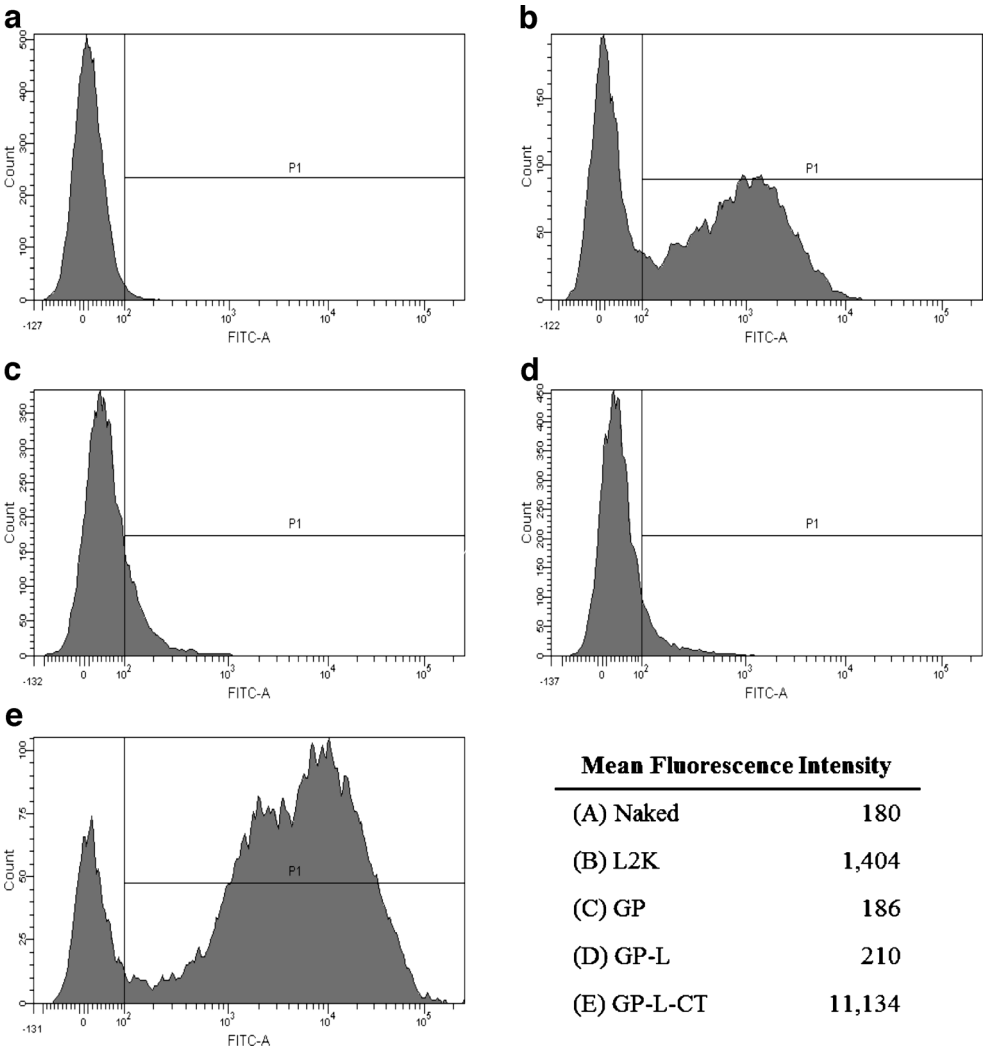

Mean Fluorescence Intensity	
(A) Naked	180
(B) L2K	1,404
(C) GP	186
(D) GP-L	210
(E) GP-L-CT	11,134

Fig. 6 *In vitro* cellular uptake efficiency of the nanocomplexes in PC-3 cells. Fluorescent siRNA was loaded into various nanocomplex formulations and fluorescence intensity measured by flow cytometry after incubating for 24 h. Plots are presented of cell count and fluorescence intensity from (**a**) naked siRNA (Naked), (**b**) siRNA/Lipofectamine 2000 (L2K), (**c**) siRNA/protamine (GP), (**d**) siRNA/protamine/lecithin (GP-L), and (**e**) siRNA/protamine/lecithin/chitosan/TPP (GP-L-CT).

be the most appropriate nanocomplex for the systemic delivery of SVN siRNA for cancer therapy. Stability of the siRNA nanocomplex in serum was ensured only in the hybrid nanocomplex, GP-L-CT, by pre-complexing with protamine (24–26) and incorporation of lecithin. Moreover, gene silencing and cellular uptake efficiencies were highly induced by complexing with chitosan and TPP (29), without interference of stabilizing components, protamine and lecithin, used in intermediate steps of the hybid nanocomplex preparation. Therefore, GP-L-CT was selected and evaluated as the final formulation in *in vivo* studies.

In Vivo NIRF Imaging and Anti-Tumor Efficacy

Tumor targetability of Cy5.5-siRNA-loaded GP-L-CT was investigated by *in vivo* NIRF imaging in a PC-3 tumor xenograft mouse model. Fluorescence intensity in the tumor region was scanned 2 and 5 h after intravenous injection, according to the previous study (32). As shown in Fig. 7, fluorescence intensity in the tumor region of Cy5.5-siRNA-loaded GP-L-CT was the highest of the experimental groups. Fluorescence intensities of the naked Cy5.5-siRNA and Cy5.5-siRNA loaded L2K were lower than that of GP-L-CT, suggesting that naked siRNA and L2K were inappropriate for systemic administration due to their low stability and delivery effect in biological fluids. Normal vasculature has a packed structure with a pore size <10 nm, however, neovasculature in the tumor region has an abnormally aligned endothelium with wide fenestrations with a pore size of 100–700 nm and defective lymphatic drainage (37). As a result, *in vivo* stabilized and circulating nano-sized drug delivery systems can easily permeate and accumulate in the tumor region. This phenomenon is known as the enhanced permeability and retention (EPR) effect, which explains the *in vivo* stability and tumor targetability of GP-L-CT. The EPR effect observed in Cy5.5-siRNA loaded GP-L-CT demonstrated that GP-L-CT was circulated in the

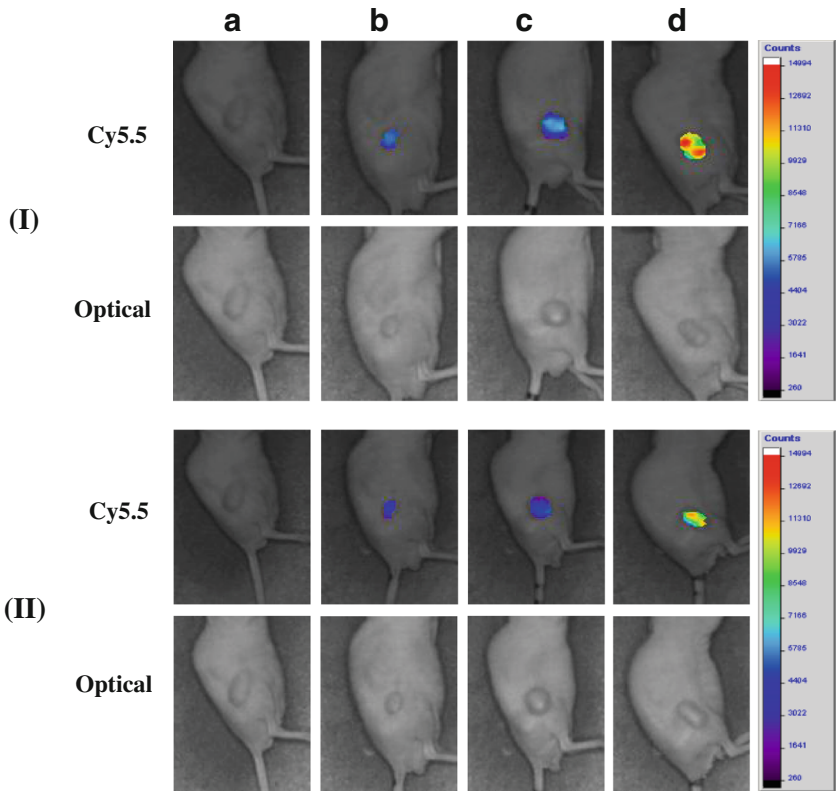

Fig. 7 *In vivo* NIRF images of siRNA-loaded nanocomplex formulations in a PC-3 tumor-xenograft mouse model. Cy5.5-filtered and optical images of tumor in (**a**) control, (**b**) naked Cy5.5-siRNA, (**c**) Cy5.5-siRNA/Lipofectamine 2000 (Cy5.5-siRNA loaded L2K), (**d**) Cy5.5-siRNA/protamine/lecithin/chitosan/TPP complex (Cy5.5-siRNA loaded GP-L-CT) groups 2 h (I) and 5 h (II) post-intravenous injection.

bloodstream and permeated into the tumor tissue as a nano-sized drug delivery system after intravenous injections.

In vivo anti-tumor efficacy of GP-L-CT nanocomplexes was tested in a PC-3 tumor xenograft mouse model by monitoring tumor growth inhibition (Fig. 8). Luciferase siRNA was incorporated into GP-L-CT for the irrelevant siRNA group. In our preliminary study, naked siRNA did not have any anti-tumor efficacy in a PC-3 tumor-bearing mouse model (data not shown). The mean tumor volumes of the PBS (control), Luciferase siRNA GP-L-CT, and SVN siRNA GP-L-CT treated groups were 615, 550, and 226 mm^3 at day 14, and 754, 742, and 277 mm^3 at day 18, respectively. The growth inhibition rate of GP-L-CT was calculated to be 75.5% at day 18 compared to the control group. It is particularly notable that the tumor volume of the SVN siRNA GP-L-CT group was significantly smaller than those of the control and Luciferase siRNA GP-L-CT groups ($P<0.05$). This indicated that anti-tumor efficacy was induced by *in vivo* systemic siRNA delivery of the chitosan-based hybrid nanocomplex.

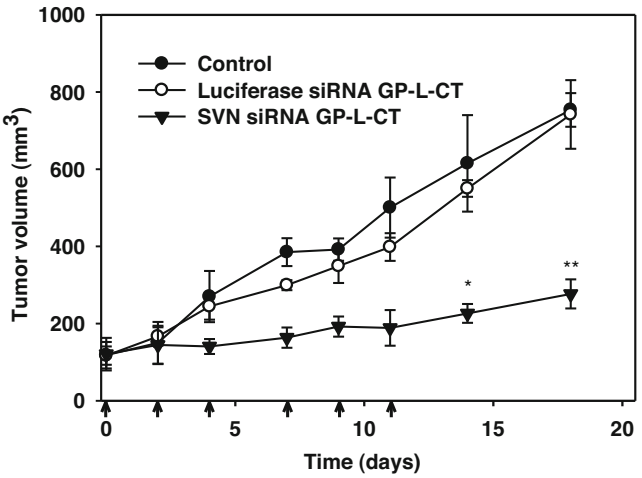

Fig. 8 *In vivo* anti-tumor efficacy of siRNA-loaded nanocomplex in a PC-3 tumor-xenograft mouse model. Tumor volume profiles of PBS (Control), luciferase siRNA/protamine/lecithin/chitosan/TPP (Luciferase siRNA GP-L-CT), SVN siRNA/protamine/lecithin/chitosan/TPP complex (SVN siRNA GP-L-CT). Nanocomplexes were injected intravenously six times for 2 weeks. $*P<0.05$ and $**P<0.01$ are established between Luciferase siRNA GP-L-CT and SVN siRNA GP-L-CT. Data represent means ± SD ($n\geq3$).

Based on its tumor targetability and anti-tumor efficacies, GP-L-CT can circulate in the bloodstream and exhibit an EPR effect with systemic administration, resulting in reduced tumor growth in a tumor xenograft mouse model. Although chitosan could be used as a cationic polymer for *in vitro* gene transfection, it is difficult to verify its *in vivo* performance due to its weakened binding affinity with nucleic acids and the aggregation that was resulted from interaction with endogenous components (17–19, 22). The significance of this study is that it identified a method for systemic application of the GP-L-CT formulation in cancer therapy and diagnosis, overcoming difficulties with instability of conventional cationic nanoparticles under physiological conditions using the hybrid nanocomplex system. Although further investigation is needed

to fully elucidate the specific mechanism and detailed *in vivo* efficacy of the developed nanocomplex, its feasibility as a nano-sized vehicle for systemic application of siRNA therapeutics was verified.

CONCLUSIONS

The low cytotoxicity, high biocompatibility, high mucoadhesiveness, and high cell permeability of chitosan have made it widely used for the delivery of nucleic acid therapeutics. However, a reduction in its *in vivo* gene delivery efficiency must be overcome. In this study, a pre-complex based on siRNA and protamine was formed and lecithin, chitosan, and TPP were added to develop a more stable and efficient hybrid nanocomplex (GP-L-CT). GP-L-CT provided suitable physicochemical properties with a positive zeta potential in DW and mean diameter <200 nm in 50% FBS for intravenous injection of siRNA, as well as superior *in vitro* cellular uptake and gene silencing efficiencies. Furthermore, systemic administration of GP-L-CT improved *in vivo* tumor targetability and anti-tumor efficacy in a tumor xenograft mouse model compared to other formulations. This novel chitosan-based hybrid nanocomplex was successfully developed for the systemic delivery of SVN siRNA, which could serve as an alternative to cationic polymeric nanoparticles that are unstable in serum.

ACKNOWLEDGMENTS AND DISCLOSURES

This work was supported by the Ministry of Knowledge Economy of Korea (10030044, SM. Noh).

REFERENCES

1. Davaa E, Ahn IH, Kang BS, Lee SE, Myung CS, Park JS. Preliminary study to determine the optimal conditions for the simultaneous complexation of siRNA and plasmid DNA. J Pharm Invest. 2013;43:499–505.
2. Wang J, Lu Z, Wientjes MG, Au JL-S. Delivery of siRNA therapeutics: barriers and carriers. AAPS J. 2010;12:492–503.
3. Behlke MA. Progress towards *in vivo* use of siRNAs. Mol Ther. 2006;13:644–70.
4. Whitehead KA, Langer R, Anderson DG. Knocking down barriers: advances in siRNA delivery. Nat Rev Drug Discov. 2009;8:129–38.
5. Zhang S, Zhao Y, Zhi D, Zhang S. Non-viral vectors for the mediation of RNAi. Bioorg Chem. 2012;40:10–8.
6. Khalil IA, Kogure K, Akita H, Harashima H. Uptake pathways and subsequent intracellular trafficking in nonviral gene delivery. Pharmacol Rev. 2006;58:32–45.
7. Ping Y, Liu C, Zhang Z, Liu KL, Chen J, Li J. Chitosan-graft-(PEI-β-cyclodextrin) copolymers and their supramolecular PEGylation for DNA and siRNA delivery. Biomaterials. 2011;32:8328–41.
8. Singha K, Namgung R, Kim WJ. Polymers in small-interfering RNA delivery. Nucleic Acid Ther. 2011;21:133–47.
9. Mao S, Sun W, Kissel T. Chitosan-based formulations for delivery of DNA and siRNA. Adv Drug Deliv Rev. 2010;62:12–27.
10. Malmo J, Hanne S, Vårum KM, Strand SP. SiRNA delivery with chitosan nanoparticles: molecular properties favoring efficient gene silencing. J Control Release. 2012;158:261–8.
11. Techaarpornkul S, Wongkupasert S, Opanasopit P, Apirakaramwong A, Nunthanid J, Ruktanonchai U. Chitosan-mediated siRNA delivery *in vitro*: effect of polymer molecular weight, concentration and salt forms. AAPS PharmSciTech. 2010;11:64–72.
12. Park S, Jeong EJ, Lee J, Rhim T, Lee SK, Lee KY. Preparation and characterization of nonaarginine-modified chitosan nanoparticles for siRNA delivery. Carbohydr Polym. 2013;92:57–62.
13. Fernandes JC, Qiu X, Winnik FM, Benderdour M, Zhang X, Dai K, *et al.* Low molecular weight chitosan conjugated with folate for siRNA delivery *in vitro*: optimization studies. Int J Nanomedicine. 2012;7:5833–45.
14. Malhotra M, Tomaro-Duchesneau C, Prakash S. Synthesis of TAT peptide-tagged PEGylated chitosan nanoparticles for siRNA delivery targeting neurodegenerative diseases. Biomaterials. 2013;34:1270–80.
15. Han HD, Mangala LS, Lee JW, Shahzad MM, Kim HS, Shen D, *et al.* Targeted gene silencing using RGD-labeled chitosan nanoparticles. Clin Cancer Res. 2010;16:3910–22.
16. Malhotra M, Lane C, Tomaro-Duchesneau C, Saha S, Prakash S. A novel method for synthesizing PEGylated chitosan nanoparticles: strategy, preparation, and *in vitro* analysis. Int J Nanomedicine. 2011;6:485–94.
17. Karmali PP, Simberg D. Interactions of nanoparticles with plasma proteins: implication on clearance and toxicity of drug delivery systems. Expert Opin Drug Deliv. 2011;8:343–57.
18. Radomski A, Jurasz P, Alonso-Escolano D, Drews M, Morandi M, Malinski T, *et al.* Nanoparticle-induced platelet aggregation and vascular thrombosis. Br J Pharmacol. 2005;146:882–93.
19. Dobrovolskaia MA, Aggarwal P, Hall JB, McNeil SE. Preclinical studies to understand nanoparticle interaction with the immune system and its potential effects on nanoparticle biodistribution. Mol Pharm. 2008;5:487–95.
20. Matsuura M, Yamazake Y, Sugiyama M, Kondo M, Ori H, Nango M, *et al.* Polycation liposome-mediated gene transfer *in vivo*. Biochim Biophys Acta. 2003;1612:136–43.
21. Ragelle H, Vandermeulen G, Préat V. Chitosan-based siRNA delivery systems. J Control Release. 2013;172:207–18.
22. Xu S, Dong M, Liu X, Howard KA, Kjems J, Besenbacher F. Direct force measurements between siRNA and chitosan molecules using force spectroscopy. Biophys J. 2007;93:952–9.
23. Doolittle H, Morel A, Talbot D. Survivin-directed anticancer therapies – A review of pre-clinical data and early-phase clinical trials. Eur Oncol. 2010;6:10–4.
24. Kundu AK, Chandra PK, Hazari S, Pramar YV, Dash S, Mandal TK. Development and optimization of nanosomal formulations for siRNA delivery to the liver. Eur J Pharm Biopharm. 2012;80:257–67.
25. Delgado D, Pozo- Rodríguez A, Solinís MA, Rodríguez-Gascón A. Understanding the mechanism of protamine in solid lipid nanoparticle-based lipofection: The importance of the entry pathway. Eur J Pharm Biopharm. 2011;79:495–502.
26. DeLong RK, Akhtar U, Sallee M, Parker B, Barber S, Zhang J, *et al.* Characterization and performance of nucleic acid nanoparticles combined with protamine and gold. Biomaterials. 2009;30:6451–9.
27. Li S, Huang L. *In vivo* gene transfer via intravenous administration of cationic lipid–protamine–DNA (LPD) complexes. Gene Ther. 1997;4:891–900.

28. Yuan H, Zhang W, Du Y, Hu F. Ternary nanoparticles of anionic lipid nanoparticles/protamine/DNA for gene delivery. Int J Pharm. 2010;392:224–31.
29. Rojanarata T, Opanasopit P, Techaarpornkul S, Ngawhirunpat T, Ruktanonchai U. Chitosan-thiamine pyrophosphate as a novel carrier for siRNA delivery. Pharm Res. 2008;25:2807–14.
30. Crawford R, Dogdas B, Keough E, Haas RM, Wepukhulu W, Krotzer S, *et al.* Analysis of lipid nanoparticles by Cryo-EM for characterizing siRNA delivery vehicles. Int J Pharm. 2011;403: 237–44.
31. Mayen V, Wutikhun T, Ketchart O, Kopermsub P. Adsorption of siRNA into mesoporous silica nanoparticles. J Microsc Soc Thai. 2012;5:10–3.
32. Cho HJ, Yoon HY, Koo H, Ko SH, Shim JS, Lee JH, *et al.* Self-assembled nanoparticles based on hyaluronic acid-ceramide (HA-CE) and Pluronic® for tumor-targeted delivery of docetaxel. Biomaterials. 2011;31:7181–90.
33. Kalsin AM, Kowalczyk B, Smoukov SK, Klajn R, Grzybowski BA. Ionic-like behavior of oppositely charged nanoparticles. J Am Chem Soc. 2006;128:15046–7.
34. Suh MS, Shim G, Lee YH, Han SE, Yu YH, Choi Y, *et al.* Anionic amino acid-derived cationic lipid for siRNA delivery. J Control Release. 2009;140:268–76.
35. Sternberg B, Hong K, Zheng W, Papahadjopoulos D. Ultrastructural characterization of cationic liposome-DNA complexes showing enhanced stability in serum and high transfection activity *in vivo*. Biochim Biophys Acta. 1998;1375:23–35.
36. Han SE, Kang H, Shim GY, Suh MS, Kim SJ, Kim JS, *et al.* Novel cationic cholesterol derivative-based liposomes for serum-enhanced delivery of siRNA. Int J Pharm. 2008;353:260–9.
37. Juliano R, Bauman J, Kang H, Ming X. Biological barriers to therapy with antisense and siRNA oligonucleotides. Mol Pharm. 2009;6:685–95.